HHS Public Access

Author manuscript

Chem Biol. Author manuscript; available in PMC 2019 June 20.

Published in final edited form as:

Chem Biol. 2015 May 21; 22(5): 593–603. doi:10.1016/j.chembiol.2015.04.016.

The effect of detergent, temperature and lipid on the oligomeric state of MscL constructs: Insights from mass spectrometry

Eamonn Reading[1], **Troy A. Walton**[2,4], **Idlir Liko**[1], **Michael T. Marty**[1], **Arthur Laganowsky**[1,3], **Douglas C. Rees**[2], and **Carol V. Robinson**[1]

[1]Department of Chemistry, Physical & Theoretical Chemistry Laboratory, University of Oxford, Oxford, UK

[2]Division of Chemistry and Chemical Engineering 114-96, Howard Hughes Medical Institute, California Institute of Technology, Pasadena, CA 91125 USA

[3]Present address: Center for Infectious and Inflammatory Diseases, Institute of Biosciences and Technology, Texas A&M Health Sciences Center, Houston, TX 77030 USA

[4]Present address: Beyond Meat, El Segundo, CA 90245 USA

Summary

The mechanosensitive channel of large conductance (MscL) acts as an emergency release valve for osmotic shock of bacteria preventing cell lysis. The large pore size, essential for function, requires the formation of oligomers with tetramers, pentamers or hexamers observed depending on the species and experimental approach. We applied non-denaturing (native) mass spectrometry to five different homologs of MscL to determine the oligomeric state under more than 50 different experimental conditions elucidating lipid binding and subunit stoichiometry. We found equilibrium between pentameric and tetrameric species that can be altered by detergent, disrupted by binding specific lipids, and perturbed by increasing temperature (37 °C). We also established the presence of lipopolysaccharide bound to MscL and other membrane proteins expressed in *Escherichia coli*, revealing a potential source of heterogeneity. More generally we highlight the use of mass spectrometry in probing membrane proteins under a variety of detergent-lipid environments relevant to structural biology.

Introduction

Mechanosensitive channels of large conductance (MscL) act as emergency non-selective release valves, for bacteria, when under high internal cellular pressures caused by hypo-osmotic shock (Booth et al., 2007; Haswell et al., 2011; Iscla and Blount, 2012; Kung et al., 2010). MscL responds to the tension of the bilayer by opening and closing its channel through a progression of subconductance states, until sufficient tension is experienced to stabilize the fully open state. The monomeric subunits of MscL are relatively small

Contact: carol.robinson@chem.ox.ac.uk.

Author Contributions

E.R., T.A.W., I.L. and A.L. performed the experiments and analyzed the data. E.R., T.A.W., A.L., D.C.R, and C.V.R designed the study. M.T.M. developed the deconvolution software and provided analysis support for this study. E.R. and C.V.R. wrote the paper with contributions from all other authors.

(*Staphylococcus aureus* (Sa) MscL, *Escherichia coli* (Ec) MscL and *Mycobacterium tuberculosis* (Mt) MscL have 120, 136 and 151 residues respectively), and possess only two trans-membrane helices (TMH) per subunit (Figure 1). It has been appreciated from the initial discovery of MscL (Sukharev et al., 1994) that the channel must be oligomeric; since the dimensions of the pore and hence conductance reflects the number of subunits, determination of the oligomeric state of MscL is crucial to understand the physiology.

The oligomeric state of MscL has been studied by a range of experimental approaches and has been observed to be tetrameric, pentameric or hexameric depending on the orthologue, solution conditions and experimental technique (Walton et al., 2015). The protein sequence is a key determinant, as changes to the protein construct may perturb the oligomeric state. Particular emphasis has been placed on the role of the cytoplasmic C-terminal domain (CTD) in this process (Anishkin et al., 2003; Blount et al., 1996; Walton and Rees, 2013; Yoshimura et al., 2008). The CTD consists of a helical bundle composed of the C-terminal soluble helix from each subunit. Recently the crystal structure of the EcMscL CTD was solved and biophysical characterization demonstrated that it formed stable pentamers devoid of the remaining EcMscL sequence (Walton and Rees, 2013). This suggests that the CTD may influence the oligomerisation and stability of the full-length protein. Detergent is another important parameter, and for a given construct, the observed oligomeric state can vary with changes in detergent. Moreover, the physiological function of MscL reflects an intimate coupling to the properties of the lipid bilayer (Iscla and Blount, 2012; Laganowsky et al., 2014), and changes in membrane environment can influence the gating properties of MscL (Moe et al., 2000). A specific interaction between MtMscL and phosphatidylinositol is crucial for the mechanosensitivity of this channel (Zhong and Blount, 2013). Indeed, since MscL only experiences a detergent environment when purified for *in vitro* studies, the physiological relevance of the detergent dependence of the channels oligomeric state has been questioned (Dorwart et al., 2010; Iscla et al., 2011).

To investigate the effects of these parameters on oligomeric state, we studied the MscL from five different bacterial sources, ranging from 120 to 151 residues in length (Figure 1b and Table 1). We used non-denaturing (native) mass spectrometry (MS) to reveal the oligomeric states of full-length and CTD truncation constructs in a variety of detergents, lipids, and solution temperatures. MS has been shown previously to enable determination of the mass, subunit stoichiometry, and lipid binding properties of membrane protein complexes (Barrera et al., 2009; Konijnenberg et al., 2014). Results presented here show that purification of EcMscL following established protocols (Chang et al., 1998; Liu et al., 2009) results in significant co-extraction with lipopolysaccharide (LPS) and show how co-extraction of this outer membrane lipid is common for a number of *E. coli* membrane proteins; using appropriate buffer conditions and/or detergents, however, LPS can be removed.

We then probe the interrelationships between protein subunit stoichiometry and the effects of different detergent-lipid environments. We find that while detergent can perturb the overall subunit stoichiometry, the majority of lipids investigated here did not influence the oligomeric state significantly. The effects of C-terminal truncations, however, showed marked preference for tetrameric forms of SaMscL while the position of the tag, whether N- or C- terminal, affected the oligomeric stability in some cases with more homogenous

populations of oligomers observed for C-terminally green florescent protein histidine (C-GFP) tagged constructs.

Overall, using this experimental dataset consisting of five homologs and various constructs we explore the effects of lipid, detergent, and temperature on the population of different oligomeric forms. From more than 50 different experimental conditions we provide the most comprehensive view to date of the inter-related factors that affect the conversion and stability of MscL oligomers.

Results

Lipopolysaccharide (LPS) binds to MscL

Starting with the expression and purification of MscL from *E. coli* with a GFP and histidine tag at the C-terminus (EcMscL C-GFP), a mass spectrum was recorded from *n*-dodecyl-β-D-maltoside (DDM) under conditions optimized for the study of membrane protein complexes (Figure 2a) (Laganowsky et al., 2013). The mass spectrum reveals two overlapping charge state series at *m/z* 8000 corresponding to oligomeric species with molecular masses of 235.2 and 238.8 kDa. Overlapping charge state series at *m/z* 2000 are also observed corresponding to monomeric subunits with molecular masses 44.0 and 14.8 kDa. The former closely matches the expected mass for this construct while the latter surprisingly corresponds to that for the native EcMscL (the subsequent use of an *E. coli* strain knocking out the native gene (Laganowsky et al., 2014) eliminated this species). The oligomer peaks must correspond to EcMscL pentamers (expected molecular mass 220.4 kDa) but there is a significant discrepancy of additional 14.8 and 18.5 kDa mass, respectively (Figure 2a). Performing this experiment on MtMscL C-GFP also revealed bound adducts with a clear additional mass in the range of 3.4–3.7 kDa from the *apo* form of MtMscL C-GFP, particularly evident in the stripped oligomer region of the mass spectrum (*m/z* 10,000 to 22,000) (Figure 2b). This suggests that MscL membrane proteins co-purify with varying amount of adducts possessing masses in the range of 3.4–3.7 kDa. Although the mass of the adduct does not define its chemical identity, the absence of charge on the bound adduct narrows down the possible candidates to either a small peptide or lipid-like molecule.

A series of experiments were performed to identify the non-covalently bound adduct with a mass ranging from 3.4–3.7 kDa. First, we did not observe a lower molecular weight band in SDS-PAGE stained with Coomassie blue dye (Figure S1), suggesting this adduct was a non-protein species. We suspected that the adduct could be the main outer membrane lipid, lipopolysaccharide (LPS). LPS has a complex and heterogeneous structure; in laboratory *E. coli* K-12 strains, LPS consists of Lipid A with two Kdo sugars and a R-core oligosaccharide domain consisting of 6 to 10 sugars (hexoses and heptoses, along with side chain modifications) corresponding to a molecular mass of ~3.4 – 4.1 kDa (Raetz, 1996). Since LPS may be detected by silver staining (Tsai and Frasch, 1982), we repeated the SDS-PAGE electrophoresis but this time followed by silver staining. A dark band appeared for a molecular species consistent with our observed adduct mass and migrating similarly to the purified LPS from *E. coli* (Figure S1). The ligand identity as LPS was further validated by dot blot analysis of purified MscL protein with an anti-Lipid A antibody (Figure S1). In addition, we expressed and purified MtMscL C-GFP from a ClearColi® *E. coli* (Lucigen), a

strain which harbors several gene knockouts that reduce the biochemical pathway of LPS to a precursor, lipid IV_A. Recording a mass spectrum of adducts bound to the MscL complex isolated from this strain reveals adducts of 1.4 kDa consistent with the mass of lipid IV_A (1409 Da) (Figure 2c). These experiments identify the bound adduct as LPS and provide an explanation for the range in mass observed for the bound adduct, due to the heterogeneity of the core oligosacchride of LPS.

To determine if LPS co-purifies with other membrane proteins, or is enhanced with MscL, we expressed and purified three additional inner membrane proteins in *E. coli* (Figure S2). Following extensive purification we found LPS bound to ~50% of the chloride channel (ClcA) and the multidrug resistance protein (MdtE), and up to ~20 % of the acriflavine resistance protein B (AcrB). We conclude that LPS binding is not specific to MscL but can occur readily to a variety of membrane proteins expressed in *E. coli* and likely goes unnoticed in typical evaluation for purity and heterogeneity (Drew et al., 2008; Gutmann et al., 2007).

To assess the stability and stoichiometry of the *apo* protein and the effects of other lipids using non-denaturing mass spectrometry, we developed purification methods for the removal of LPS. Inspired by the use of Triton X-100 in removing LPS from outer membrane proteins (de Cock et al., 1996; Magalhaes et al., 2007) mass spectra of MtMscL-GFP extracted with 1% Triton X-100 were obtained revealing small fractions of LPS bound to the protein complex and oligomer stripped species. In the presence of 1% Triton X-100, but this time with the addition of 20% glycerol, a dramatic increase in the proportion of LPS bound to the complex was observed. Interestingly substitution of Triton X-100 with octyl glucose neopentyl glycol (OGNG) detergent in glycerol-free buffer resulted in no detectable LPS bound to the complex (Figure S3). We conclude therefore that LPS removal is dependent on the physical properties of the detergent and that, in this case, OGNG is more efficient in removing this adduct from MtMscL than other detergents that we tested.

MscL stoichiometry in different detergents

To probe the dependence of the oligomeric states of MscL within different detergents, we compared two structurally characterized homologs, SaMscL and MtMscL. When in a DDM environment, we found that the N-terminally histidine tagged (N-His) SaMscL was tetrameric (47%) with smaller oligomers present (trimers, dimers and monomers), while N-His MtMscL showed a significant population of pentamers (38%) and tetramers (63%) (Figure 3). In the same DDM detergent environment, but with a C-terminal GFP histidine tag (C-GFP), SaMscL and MtMscL both formed stable pentamers (100%). Furthermore, the C-GFP constructs of EcMscL, *A. ferrooxidans* (Af) MscL and *T. thermophilus* (Tt) MscL, all produced exclusively pentameric complexes in DDM (Figure 3).

To determine if there was a dependence on detergent and oligomeric state, we then compared SaMscL and MtMscL constructs in three further detergents: octyl-β-D-glucopyranoside (OG), tetraethylene glycol monooctyl ether (C8E4) and lauryldimethyl amine oxide (LDAO). Interestingly, we found that N-His SaMscL, N-His MtMscL, SaMscL C-GFP, and MtMscL C-GFP in LDAO, OG and C8E4 was exclusively pentameric, with small populations of GFP truncated species observed in some cases. Taken together, this

demonstrates that the protein construct can influence the observed oligomer distributions, with full-length SaMscL and MtMscL C-GFP constructs producing pentameric states predominantly, while the N-terminal histidine modifications can destabilize pentameric forms in one of the detergents investigated here.

The effects of the C-terminal domain on the oligomeric state

Given previous observations that the C-terminal domain (CTD) of MtMscL and EcMscL have extensive inter-subunit interactions (Chang et al., 1998; Walton and Rees, 2013) and the proposal that these interactions may control the oligomeric state we generated SaMscL and MtMscL constructs (C-GFP and N-His) in which we deleted these C-terminal amino acid residues (CΔ) (Table 1). We found that these truncations had little or no effect on MtMscL in the detergents DDM and LDAO, with MtMscL CΔ49 C-GFP remaining predominantly pentameric; however the presence of C8E4, and OG especially, disrupted the MtMscL CΔ49 C-GFP pentamer into smaller oligomers (Figure 3).

By contrast SaMscL CΔ25 C-GFP revealed almost exclusive populations of the tetrameric species in the same conditions (Figure 3). To assess the possible effects of the C-GFP on the stability of SaMscL oligomers we investigated the N-His SaMscL CΔ26 in addition to the C-GFP. We found that this construct produced a mixture of oligomeric states in DDM with no pentameric channel present, similar to that observed for the full-length construct with the N-His tag. Interestingly, N-His SaMscL CΔ26 produced an almost 80:20 population of pentamer: tetramer in LDAO consistent with OCAM and crystallographic results, but in contrast to the full-length protein where only pentamer was observed. Additionally we observed that the CTD truncated species of SaMscL and MtMscL in the presence of particular detergents were not compatible with mass spectrometry analysis, producing unresolvable mass spectra through aggregation, insolubility or degradation, whether N or C-terminally tagged (pink boxes, Figure 3). This was indeed the case for the N-His MtMscL CΔ49 construct where data was unobtainable in all detergents examined here.

Tetramers were observed however almost exclusively for the SaMscL CΔ25 C-GFP construct in LDAO, DDM and C8E4. Interestingly only pentamers were seen for the full-length protein from equivalent conditions. We can conclude therefore that truncation of these C-terminal residues caused all SaMscL CΔ constructs to form populations of tetramers in contrast to the pentameric full length constructs. This is in accordance with the crystal structure of the SaMscL tetramer purified and crystallized in LDAO (Liu et al., 2009) as well as analytical ultra-centrifugation (AUC) data from the same solution conditions (Dorwart et al., 2010).

Influence of temperature on MscL oligomeric state

Our observation that SaMscL populates various oligomeric states according to the construct and the detergent environment implies that different oligomeric forms can interconvert. Reasoning that an increase in temperature could promote this interconversion we incubated and equilibrated solutions of SaMscL C-GFP in both LDAO and C8E4 for periods of up to one hour at 4 °C or 37 °C prior to mass spectrometry analysis (Figure 4). Following incubation at 4 °C SaMscL C-GFP was solely pentameric in both LDAO and C8E4.

Interestingly when equilibrated at 37 °C, for one hour, SaMscL C-GFP remained exclusively pentameric in C8E4. By contrast the same construct underwent complete conversion to a tetramer in LDAO following incubation at the same elevated temperature. When the LDAO solution at 37 °C was then re-equilibrated to 4 °C, SaMscL C-GFP precipitated. This would imply that the oligomeric switch from pentamer to tetramer at elevated temperature is irreversible, at least in LDAO.

Together these results reflect a relationship between temperature and oligomeric state in one of the two detergent environments studied here. The fact that the pentameric complex was perturbed in LDAO, but not in C8E4, likely reflects the different oligomeric stabilities of SaMscL in these two detergent environments.

Influence of lipids on the inter-conversion between SaMscL oligomers

Given the observation that SaMscL constructs are able to form stable tetramers and pentamers in solution and can convert from pentamers to tetramers following thermal activation, the potential influence of lipids on this interconversion was investigated. Different lipids were added to SaMscL constructs solubilized in either LDAO or C8E4 (Figure 5). The lipid composition of the Sa membrane mainly consists of cardiolipin (CDL), phosphatidylglycerol (PG) and lysyl-PG in relative populations of approximately 24, 10 and 50 %, respectively (Koch et al., 1984). These lipids and the lipid phosphatidylethanolamine (PE), which is non-natural to the Sa membrane, were therefore added to full-length SaMscL C-GFP in LDAO and C8E4, and incubated for 6 h at 4 °C, to investigate the effect of natural and non-natural lipids on MscL oligomeric state.

In the LDAO-lipid environments, the predominant pentameric oligomer was retained with a small amount of conversion to tetrameric forms observed for each lipid. The highest population of tetrameric SaMscL C-GFP was observed with CDL and Lysyl-PG (23% and 21% respectively). For the C-terminal truncation SaMscL CΔ25 C-GFP, the addition of lipid had little influence on the oligomeric state, the tetramer forming exclusively in LDAO as seen previously in the absence of lipids (Figure 3). When assessing the effects of the four different lipids in C8E4 on the stability of full-length SaMscL C-GFP we found that it retained its pentameric form, as observed in the absence of added lipids (Figure 3). However the SaMscL CΔ25 C-GFP in C8E4 generated predominantly tetrameric forms of the protein with a small population of pentamer observed. For the SaMscL CΔ25 C-GFP construct, the population of pentamer in the presence of CDL, PG and PE lipids (16%, 19%, and 19%, respectively) is greater than in C8E4 alone (10%) implying that lipids can stabilize the pentameric state of SaMscL within the C8E4 detergent.

Given that lipids may play a role in stabilizing these different oligomers, we then investigated the effects of lipid on the temperature-induced (37 °C) inter-conversion probed above (Figure 6). Full-length SaMscL, cleaved of its C-terminal GFP tag, in LDAO was doped with lipids at 4 °C for 12 hours and revealed mainly pentameric and tetrameric complexes in accordance with the observations for a detergent-only environment. However substantially less pentamer was observed for detergent-lipid solutions (detergent-only = 87% and lipid-detergent = 19–58%). Similar populations of pentamer and tetramer were observed with PG, lysyl-PG and PE. CDL did not follow the same trend, however producing

substantially less pentamer (19%) and forming moderate populations of trimer (27%). Incubating at 37 °C for 12 hours, however, caused SaMscL to form tetramers and trimers but no pentamers irrespective of the lipid added. Surprisingly, all lipids caused an increase in lower oligomeric species in comparison to the LDAO-only environment. This suggests that lipids can affect populations of oligomers for SaMscL in the presence of LDAO detergent. Since conversion from pentamers to tetramers occurs more readily in LDAO than in C8E4, and given that CDL was the most effective in causing this transition, but was less effective than the detergent environment, we conclude that the dominant effect on oligomeric stability is therefore the detergent environment.

Discussion

We have shown using non-denaturing mass spectrometry that the detergent or detergent-lipid environment can influence the oligomeric states of MscL channels. However to assess the effects of lipids and detergents on subunit stoichiometry it was critical that protein preparations are lipid-free initially. In this regard, knowledge that MscL co-purifies with LPS, an outer membrane lipid and endotoxin known to contaminate recombinant protein preparations from gram-negative bacteria (Morrison and Ulevitch, 1978) is critical. We also found that, rather than binding specifically to MscL, LPS also co-purifies with a number of other membrane proteins isolated from *E. coli*, adding a potential complication to biophysical/biochemical analyses. The presence of LPS if undetected could therefore complicate the analysis of the effects of exogenously added lipids or reconstitution, especially in the case of patch clamp experiments for MscL or crystallization experiments.

Although pentameric channels are observed under many conditions for all five full-length homologues (Mt, Sa, Ec, Af and Tt) populations of lower order oligomers could be seen depending on the detergent environments and tag placement. These different populations were assessed using a mass spectral deconvolution algorithm (Marty et al., 2015) revealing the relative abundance and diversity of MscL oligomeric states *in vitro*. C-GFP provided more homogenous oligomeric states compared to the N-His constructs. Truncation of the CTD of MscL channels was also found to be critical, leading to enhanced dissociation, aggregation and inter conversion to lower oligomeric states, with CTD truncated SaMscL forming tetramers within all detergent environments. This suggests that the CTD has a role in oligomeric stability. However it has previously been shown that CTD truncated and full-length SaMscL forms predominantly pentamers in native membranes (Dorwart et al., 2010; Iscla et al., 2011). Interestingly we found that the inter-conversion of full-length SaMscL from a pentamer to a tetramer could be stimulated by temperature, in a detergent dependent manner. Therefore the solubilizing detergent environment has a major influence on the oligomeric state of MscL.

Understanding the formation and inter-conversion between oligomeric states of membrane proteins enables the mechanisms for their function to be deciphered and understood. Comparing our results for MscL with the α-helical trimeric membrane protein diacylglycerol kinase (DGK), recently shown to form trimers and monomers *in vitro*; we note that DGK has high kinetic stability in OG (up to several weeks) and in liposomes at 37 °C (Jefferson et al., 2013). By contrast, SaMscL converts from pentamers to tetramers

within an hour, at 37 °C in LDAO, and can form different oligomers in DDM but does not convert when in C8E4. This further supports that MscL oligomeric state is highly sensitive to its detergent environment. Interestingly the presence of lipids affected the oligomer conversion of SaMscL. CDL was found to have a more destabilizing effect on the SaMscL pentameric state than other smaller lipids (PG, lysyl-PG and PE). It is noteworthy however that CDL, PG and lysyl-PG exist in the natural Sa membrane (Koch et al., 1984). We conclude therefore that while membrane proteins can exhibit vastly different thermodynamic and kinetic stabilities (e.g. DGK and MscL) MscL is exquisitely sensitive to its detergent-lipid environment.

Multimeric membrane proteins may possess a number of oligomeric states that are possible within the bilayer environment. It is likely that for MscL, quaternary and tertiary structural stability are dictated by the combination of physical properties of bilayers (i.e. membrane curvature, tension, charge, pressure (Booth, 2005; Phillips et al., 2009)) as well as direct lipid interactions (Bogdanov et al., 2014; Laganowsky et al., 2014; Lee, 2011). Here we have demonstrated that the solubilizing detergent environment has a dominant and profound impact on the quaternary structure (oligomeric state) of MscL channels, especially the SaMscL channel in the presence of LDAO. Therefore the solubilization of MscL from its native membrane environment can influence the oligomeric state detected. However, this destabilization could arise either from the removal of stabilizing interactions with lipids or from the loss of the physical presence of the bilayer.

For the MtMscL and SaMscL channels it has been observed that when maintained in a pentameric form, in the appropriate detergent, specific lipid interactions stabilize its tertiary structure. Interestingly however a range of lipids were found to stabilize MscL to a similar degree indicating little selectivity for particular lipid classes (Laganowsky et al., 2014, unpublished data). However while lipids stabilized the pentameric structure of SaMscL within C8E4, lipids caused destabilization when in an LDAO environment. We propose therefore that although lipids stabilize the tertiary structure of MscL they cannot prevent the dominant quaternary destabilization caused, within certain detergent environments, and by removal from their natural bilayer environment. The extent of quaternary destabilization is dependent on the homologue, construct, and detergent environment and, most importantly, how well this environment can substitute for the physical properties of native membranes. The natural bilayer possesses many different biophysical properties in comparison to a micelle, such as the greater exclusion of water as well as differences in both the profile and extent of lateral pressure. Recapitulating these attributes, in a homogeneous detergent micelle is consequently a formidable task.

The dominant factor which determines the diversity of states observed for MscL channels is therefore likely due to the kinetic stability of the various oligomers within different detergent environments. Since we can separate the effects of individual lipid binding events (Laganowsky et al., 2014) from the physical effects afforded by the physical presence of the lipid bilayer, we conclude that quaternary destabilization likely arises when the detergent micelle replaces the native membrane environment rather than as a result of delipidation. This is in accord with the evolutionary function of MscL channels, their intimate relationship with tension and pressures in the bilayers acting to open and close the non-

selective pore accordingly (Martinac, 2011; Perozo et al., 2002; Phillips et al., 2009; Sawada et al., 2012) and, as proposed here, to maintain (or change) its oligomeric state after it has been formed.

More generally the ability of non-denaturing mass spectrometry to characterize these interconverting states and compositional heterogeneity as a function of protein construct, purification conditions, detergent, lipid and applied temperature, is likely to lead to powerful insights into membrane proteins; not only to guide structural biologists but also for the many biotechnology applications of protein channels that are rapidly coming to the fore (Charalambous et al., 2012; Iscla et al., 2013; Koçer et al., 2005; Koçer et al., 2006; Yang et al., 2013).

Experimental Procedures

MscL expression and purification

MscL constructs with a C-terminal fusion to green fluorescent protein (GFP) and 6x histidine-tag constructed as previously described (Laganowsky et al., 2014). Constructs containing an N-terminal 6x histdine-tag were constructed as previously described (Chang et al., 1998; Liu et al., 2009). Plasmids were transformed into a modified *E. coli* strain (Laganowsky et al., 2014), BL21(DE3) *ΔmscL::Kan*^{R} unless otherwise stated. Proteins were expressed and purified as previously described (Chang et al., 1998; Laganowsky et al., 2014; Liu et al., 2009). To investigate the effect of detergent on MscL oligomeric state a mass spectrometry membrane protein detergent screen was performed on the constructs as previously described (Laganowsky et al., 2013).

Briefly, the protein was purified from the membranes with 2% TX-100, 1% DDM, 1% LDAO, 1.5% OG or 5% C8E4 detergent in 100 mM sodium chloride, 20% glycerol, 5 mM BME, and 20 mM TRIS, pH 7.4 at room temperature supplemented with a complete protease inhibitor tablet and incubated overnight at 4 °C with gentle agitation. Insoluble material was pelleted by centrifugation at 20,000 g for 25 minutes at 4 °C and the clarified supernatant purified using Ni-NTA agarose (Qiagen) drip columns (Bio-spin Chromatography columns, Bio-Rad). Membrane protein samples were injected onto a Superdex 200 5/150 (GE Healthcare) column equilibrated in 130 mM sodium chloride, 10% glycerol, and 50 mM TRIS, pH 7.4 at room temperature supplemented with of 2x critical micelle concentration (CMC) of the detergent of interest. Peak fractions were concentrated and buffer exchanged into MS Buffer (2x CMC detergent of interest and 200 mM ammonium acetate, pH 8.0 with ammonium hydroxide) using a centrifugal buffer exchange device (Micro Bio-Spin 6, Bio-Rad).

Lipid preparation

Lipids (Avanti Polar Lipids) were prepared and added as previously described (Laganowsky et al., 2013). Different lipids were added to MscL, solubilized in LDAO, at an empirically determined protein:lipid:detergent molar ratio in order to sustain electrospray and achieve quality mass spectra: *E. coli* L-α-phosphatidylglycerol (PG) (1:9:548), *E. coli* cardiolipin

(1:4.8:548), 1,2-dioleoyl-sn-glycero-3-[phosphor-rac-(3-lysyl(1-glycerol))] (lysyl-PG) (1:7:548), and *E.coli* L-α-phosphatidylethanolamine (PE) (1:9.5:548).

Dot blot analysis

LPS standard purchased from Sigma (L2880 from *E. coli* O55:B5) was prepared at 2.3 mg/mL in 0.5 M sodium chloride. Dot blot was performed on PVDF membranes spotted with 1ul of protein in buffer (20mM Tris pH 7.5, 150mM NaCl, 0.02% DDM). The blot was probed with primary anti-LipidA antibody (Pierce PA73178) at a 1:1000 dilution in TBST (Tris-buffered saline with Tween 20) plus 5% non-fat milk (probing/blocking were concurrent). After washing with TBST, the blot was probed with secondary anti-goat-HRP conjugate at a 1:10,000 dilution in TBST plus 5% non-fat milk. After washing with TBST, blot was developed with Western Lightening Plus ECL substrate (Perkin Elmer) for 3 minutes and film exposed for 2 min before development. All constructs were solubilized and purified at 4 °C and then flash frozen before immunodot blot analysis.

Non-denaturing mass spectrometry

A modified Q-ToF2 mass spectrometer (Micromass, Manchester, UK) with a Z-spray source (Sobott et al., 2002) was used. Typical instrument settings were 5–7 μbar source pressure, 1.5–1.8 kV capillary voltage, 150–190 V cone voltage, 1–10 V for extraction voltage, 180–200 V for collision voltage, either SF6 or argon for collision gas, and 0.2–0.3 MPa for collision gas pressure. In addition another modified Q-ToF2 was used; this instrument was modified to facilitate high-mass molecule transmission and allow for higher collision activation capabilities, as previously described (Hopper et al., 2013). The modifications were conducted by the Mass Spec Service Solutions Ltd. (MSSS). Both mass spectrometers used a multi-channel plate (MCP) detector. The accelerating voltages used were optimized so as to maintain the oligomeric state of the membrane proteins whilst removing the maximal amount of detergent or detergent-lipid. Because detergent removal is dictated by the physical properties of the detergent micelle (Reading et al. 2015) it is not possible to compare accelerating voltage conditions for constructs in different detergents. The relative abundances of oligomers were calculated using the UniDec deconvolution software program (Marty et al., 2015) with detector efficiency taken into account (Ebong et al., 2011; Fraser, 2002; Stengel et al., 2012).

Non-denaturing mass spectrometry deconvolution

Deconvolution was performed using a Bayesian deconvolution algorithm described previously (Marty et al., 2015, unidec.chem.ox.ac.uk). Mass spectra and the detail for each fit (and the fitting parameters used) is provided in Tables S1–3 and Supplemental Figures S4–10. Discriminating between native oligomers and potential collisional induced dissociation (CID) products was based on the charge states of the protein species. CID for homo-oligomers characteristically leads to the loss of highly charged monomer subunits producing charge-stripped oligomers which possess substantially lower average charge states resulting in series at high *m/z* values (Benesch et al, 2006). Additionally, a detergent dependent relationship exists between membrane protein mass and the ion charge state produced by nano-electrospray ionization (Reading et al, 2015). Together this evidence enables a distinction between native oligomeric forms and those produced by CID.

Briefly, spectral smoothing and background subtraction were applied to the data prior to deconvolution. Peak widths were determined by fitting peaks to either a Gaussian or a split Gaussian/Lorentzian model and were between 15–80 *m/z*, generally ~35, full width at half maximum (mzsig). Charge was allowed to range from 1 to 100, and mass (massub and masslb; ub = upper bound and lb = lower bound) and *m/z* range (minmz and maxmz) were limited for each data. Errors were estimated using k-fold cross validation where k is 2, 3, 4, or 5. The unprocessed data was sampled by deleting every k'th data point in k different reading frames. Each of these 14 sub-spectra were processed and fit with the same parameters. Abundances are reported as the mean and standard deviation of the peak height from these 14 fits. The pseudo intensities, intensity error derived from the deconvolution algorithm, relative oligomer abundances and propagated errors are summarized in Tables S1–3.

Supplementary Material

Refer to Web version on PubMed Central for supplementary material.

Acknowledgements

This work was supported by an ERC Advanced Investigator Award (26851) (IMPRESS), a Royal Society Research Professorship, a Medical Research Council Program Grant (98101) and an NIH grant GM084211. The authors declare no competing financial interests.

References

Anishkin A, Gendel V, Sharifi NA, Chiang CS, Shirinian L, Guy HR, and Sukharev S (2003). On the conformation of the COOH-terminal domain of the large mechanosensitive channel MscL. J. Gen. Physiol 121, 227–244. [PubMed: 12601086]

Barrera NP, Isaacson SC, Zhou M, Bavro VN, Welch A, Schaedler TA, Seeger MA, Miguel RN, Korkhov VM, van Veen HW, et al. (2009). Mass spectrometry of membrane transporters reveals subunit stoichiometry and interactions. Nat. Methods 6, 585–587. [PubMed: 19578383]

Benesch JLP, Aquilina JA, Ruotolo BT, Sobott F and Robinson CV (2006). Tandem mass spectrometry reveals the quaternary organization of macromolecular assesmblies. Chem. Biol 13, 597–605 [PubMed: 16793517]

Blount P, Sukharev SI, Schroeder MJ, Nagle SK, and Kung C (1996). Single residue substitutions that change the gating properties of a mechanosensitive channel in Escherichia coli. Proc. Natl. Acad. Sci. USA 93, 11652–11657. [PubMed: 8876191]

Bogdanov M, Dowhan W, and Vitrac H (2014). Lipids and topological rules governing membrane protein assembly. Biochim. Biophys. Acta 1843, 1475–1488. [PubMed: 24341994]

Booth IR, Edwards MD, Black S, Schumann U, and Miller S (2007). Mechanosensitive channels in bacteria: signs of closure? Nat. Rev. Microbiol 5, 431–440. [PubMed: 17505523]

Booth PJ (2005). Sane in the membrane: designing systems to modulate membrane proteins. Curr. Opin. Struc. Biol 15, 435–440.

Chang G, Spencer RH, Lee AT, Barclay MT, and Rees DC (1998). Structure of the MscL homolog from Mycobacterium tuberculosis: a gated mechanosensitive ion channel. Science 282, 2220–2226. [PubMed: 9856938]

Charalambous K, Booth PJ, Woscholski R, Seddon JM, Templer RH, Law RV, Barter LM, and Ces O (2012). Engineering de novo membrane-mediated protein-protein communication networks. J. Am. Chem. Soc 134, 5746–5749. [PubMed: 22428921]

de Cock H, van Blokland S, and Tommassen J (1996). In vitro insertion and assembly of outer membrane protein PhoE of Escherichia coli K-12 into the outer membrane. Role of Triton X-100. J. Biol. Chem 271, 12885–12890. [PubMed: 8662743]

Dorwart MR, Wray R, Brautigam CA, Jiang Y, and Blount P (2010). S. aureus MscL is a pentamer in vivo but of variable stoichiometries in vitro: implications for detergent-solubilized membrane proteins. PLoS Biol. 8, e1000555. [PubMed: 21151884]

Drew D, Newstead S, Sonoda Y, Kim H, von Heijne G, and Iwata S (2008). GFP-based optimization scheme for the overexpression and purification of eukaryotic membrane proteins in Saccharomyces cerevisiae. Nat. Protoc 3, 784–798. [PubMed: 18451787]

Ebong IO, Morgner N, Zhou M, Saraiva MA, Daturpalli S, Jackson SE, and Robinson CV (2011). Heterogeneity and dynamics in the assembly of the heat shock protein 90 chaperone complexes. Proc. Natl. Acad. Sci. USA 108, 17939–17944. [PubMed: 22011577]

Fraser GW (2002). The ion detection efficiency of microchannel plates (MCPs). Int. J. Mass Spectrom. 215, 13–30.

Gutmann DA, Mizohata E, Newstead S, Ferrandon S, Postis V, Xia X, Henderson PJ, van Veen HW, and Byrne B (2007). A high-throughput method for membrane protein solubility screening: the ultracentrifugation dispersity sedimentation assay. Protein Sci. 16, 1422–1428. [PubMed: 17567744]

Haswell ES, Phillips R, and Rees DC (2011). Mechanosensitive channels: what can they do and how do they do it? Structure 19, 1356–1369. [PubMed: 22000509]

Hopper JT, Yu YT, Li D, Raymond A, Bostock M, Liko I, Mikhailov V, Laganowsky A, Benesch JL, Caffrey M, et al. (2013). Detergent-free mass spectrometry of membrane protein complexes. Nat. Methods 10, 1206–1208. [PubMed: 24122040]

Iscla I, and Blount P (2012). Sensing and responding to membrane tension: the bacterial MscL channel as a model system. Biophys. J 103, 169–174. [PubMed: 22853893]

Iscla I, Eaton C, Parker J, Wray R, Kovacs Z, and Blount P (2013). Improving the design of a MscL-based triggered nanovalve. Biosensors 3, 171–184. [PubMed: 23678232]

Iscla I, Wray R, and Blount P (2011). The oligomeric state of the truncated mechanosensitive channel of large conductance shows no variance in vivo. Protein Sci. 20, 1638–1642. [PubMed: 21739498]

Jefferson RE, Blois TM, and Bowie JU (2013). Membrane proteins can have high kinetic stability. J. Am. Chem. Soc 135, 15183–15190. [PubMed: 24032628]

Koçer A, Walko M, Meijberg W, and Feringa BL (2005). A light-actuated nanovalve derived from a channel protein. Science 309, 755–759. [PubMed: 16051792]

Koçer A, Walko M, Bulten E, Halza E, Feringa BL, and Meijberg W (2006). Rationally designed chemical modulators convert a bacterial channel protein into a pH-sensory valve. Angew. Chem. Int. Ed 45, 3126–3130

Koch HU, Haas R, and Fischer W (1984). The role of lipoteichoic acid biosynthesis in membrane lipid metabolism of growing Staphylococcus aureus. Eur. J. Biochem 138, 357–363. [PubMed: 6697992]

Konijnenberg A, Yilmaz D, Ingolfsson HI, Dimitrova A, Marrink SJ, Li Z, Venien-Bryan C, Sobott F, and Kocer A (2014). Global structural changes of an ion channel during its gating are followed by ion mobility mass spectrometry. Proc. Natl. Acad. Sci. USA 111, 17170–17175. [PubMed: 25404294]

Kung C, Martinac B, and Sukharev S (2010). Mechanosensitive channels in microbes. Annu. Rev. Microbiol 64, 313–329. [PubMed: 20825352]

Laganowsky A, Reading E, Allison TM, Ulmschneider MB, Degiacomi MT, Baldwin AJ, and Robinson CV (2014). Membrane proteins bind lipids selectively to modulate their structure and function. Nature 510, 172–175. [PubMed: 24899312]

Laganowsky A, Reading E, Hopper JT, and Robinson CV (2013). Mass spectrometry of intact membrane protein complexes. Nat. Protoc 8, 639–651. [PubMed: 23471109]

Lee AG (2011). Biological membranes: the importance of molecular detail. Trends Biochem. Sci 36, 493–500. [PubMed: 21855348]

Liu Z, Gandhi CS, and Rees DC (2009). Structure of a tetrameric MscL in an expanded intermediate state. Nature 461, 120–124. [PubMed: 19701184]

Magalhaes PO, Lopes AM, Mazzola PG, Rangel-Yagui C, Penna TC, and Pessoa A Jr. (2007). Methods of endotoxin removal from biological preparations: a review. J. Pharm. Pharm. Sci 10, 388–404. [PubMed: 17727802]

Martinac B (2011). Bacterial mechanosensitive channels as a paradigm for mechanosensory transduction. Cell Physiol. Biochem 28, 1051–1060. [PubMed: 22178995]

Marty MT, Baldwin AJ, Marklund EG, Hochberg GK, Benesch JL, and Robinson CV (2015) Bayesian deconvolution of mass and ion mobility spectra: From binary interactions to polydisperse ensembles. Anal. Chem

Moe PC, Levin G, and Blount P (2000). Correlating a protein structure with function of a bacterial mechanosensitive channel. J. Biol. Chem 275, 31121–31127. [PubMed: 10846181]

Morrison DC, and Ulevitch RJ (1978). The effects of bacterial endotoxins on host mediation systems. A review. Am. J. Pathol 93, 526–618. [PubMed: 362943]

Perozo E, Cortes DM, Sompornpisut P, Kloda A, and Martinac B (2002). Open channel structure of MscL and the gating mechanism of mechanosensitive channels. Nature 418, 942–948. [PubMed: 12198539]

Phillips R, Ursell T, Wiggins P, and Sens P (2009). Emerging roles for lipids in shaping membrane-protein function. Nature 459, 379–385. [PubMed: 19458714]

Raetz CR (1996). Bacterial lipopolysaccharides: a remarkable family of bioactive macroamphiphiles In Escherichia coli and Salmonella: cellular and molecular biology, Neidhardt FC, Curtiss R, Ingraham JI, Lin ECC, Low KB, Magasanik B, Reznikoff W, Riley M, Schaechter M, and Umbarger HE, eds. (Washington, D.C.: ASM Press), pp. 1035–1063.

Reading E, Liko I, Allison TM, Benesch JLP, Laganowsky A, and Robinson CV (2015). The role of the detergent micelle in preserving the structure of membrane proteins in the gas phase. Angew. Chem. Int. Ed 54, 4577–4581

Sawada Y, Murase M, and Sokabe M (2012). The gating mechanism of the bacterial mechanosensitive channel MscL revealed by molecular dynamics simulations: from tension sensing to channel opening. Channels (Austin, Tex) 6, 317–331.

Sievers F, Wilm A, Dineen D, Gibson TJ, Karplus K, Li W, Lopez R, McWilliam H, Remmert M, Soding J, et al. (2011). Fast, scalable generation of high-quality protein multiple sequence alignments using Clustal Omega. Mol. Syst. Biol 7, 539. [PubMed: 21988835]

Sobott F, Hernandez H, McCammon MG, Tito MA, and Robinson CV (2002). A tandem mass spectrometer for improved transmission and analysis of large macromolecular assemblies. Anal. Chem 74, 1402–1407. [PubMed: 11922310]

Stengel F, Baldwin AJ, Bush MF, Hilton GR, Lioe H, Basha E, Jaya N, Vierling E, and Benesch JL (2012). Dissecting heterogeneous molecular chaperone complexes using a mass spectrum deconvolution approach. Chem. Biol 19, 599–607. [PubMed: 22633411]

Sukharev SI, Blount P, Martinac B, Blattner FR, and Kung C (1994). A large-conductance mechanosensitive channel in E. coli encoded by mscL alone. Nature 368, 265–268. [PubMed: 7511799]

Tsai C-M, and Frasch CE (1982). A sensitive silver stain for detecting lipopolysaccharides in polyacrylamide gels. Anal. Biochem 119, 115–119. [PubMed: 6176137]

Walton TA, Idigo CA, Herrera N, and Rees DC (2015). MscL: channeling membrane tension. Pflugers Arch. 467, 15–25. [PubMed: 24859800]

Walton TA, and Rees DC (2013). Structure and stability of the C-terminal helical bundle of the E. coli mechanosensitive channel of large conductance. Protein Sci. 22, 1592–1601. [PubMed: 24038743]

Yang Y, Liu R, Xie H, Hui Y, Jiao R, Gong Y, and Zhang Y (2013). Advances in nanopore sequencing technology. J. Nanosci. Nanotechnol 13, 4521–4538. [PubMed: 23901471]

Yoshimura K, Usukura J, and Sokabe M (2008). Gating-associated conformational changes in the mechanosensitive channel MscL. Proc. Natl. Acad. Sci. USA 105, 4033–4038. [PubMed: 18310324]

Zhong D, and Blount P (2013). Phosphatidylinositol Is Crucial for the Mechanosensitivity of Mycobacterium tuberculosis MscL. Biochemistry 52, 5415–5420. [PubMed: 23875651]

Significance

Mechanosensitive channels are membrane proteins that are present within all organisms and are of great significance since they control mechanical sensation. The bacterial mechanosensitive channel of large conductance (MscL) is important for the maintenance of cell turgor, acting as an emergency solute release valve when under hypo-osomotic stress. Additionally, MscL has been tailored for use in nanotechnology – for example as a nanovalve or in building protein-protein communication networks. MscL acts in concert with its lipid environment during channel opening (and closing). The size of its pore, and therefore its function, is determined by the oligomeric state of the channel. However, the oligomeric state has been highly controversial since it has been observed in tetrameric, pentameric and hexameric forms. Critical in the field, therefore, is the question as to whether or not these oligomers can interconvert *in vitro* in response to different lipid and/or detergent environments. To address this important question we have investigated more than 50 different experimental conditions in which we varied both the protein construct and detergent/lipid environments. We then exploited non-denaturing mass spectrometry's unrivalled ability to monitor both protein subunit stoichiometry and lipid binding simultaneously to address the question of their oligomeric states. Here we demonstrate how this biophysical tool, coupled with state of the art de-convolution algorithms, can be used to probe the equilibria between different oligomeric states of membrane protein complexes and demonstrate an exquisite sensitivity of MscL oligomers to temperature and the detergent/lipid environment.

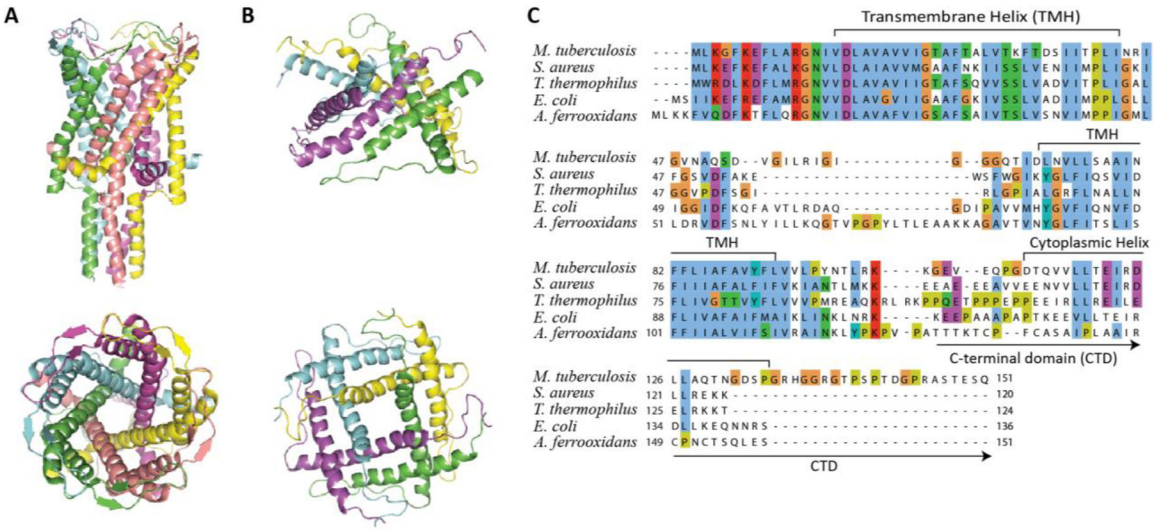

Figure 1.

Structures and sequence alignment of mechanosensitive channels of large conductance. Side (Top) and top (Bottom) views of the crystal structures of pentameric MtMscL (**a**, PDB = 2OAR) and tetrameric SaMscL CΔ26 (**b**, PDB = 3HZO). **c**, Amino acid sequence alignment for MscL homologs produced using the CLUSTAL Omega program (Sievers et al., 2011). Amino acids are colored according to the Clustal X color scheme. Accession numbers of the sequences used for alignments are: *E. coli* = POA742, *M. tuberculosis* = A5U127, *S. aureus* = P68805, *A. ferrooxidans* = B5ERJ9, and *T. thermophilus* = Q72L04.

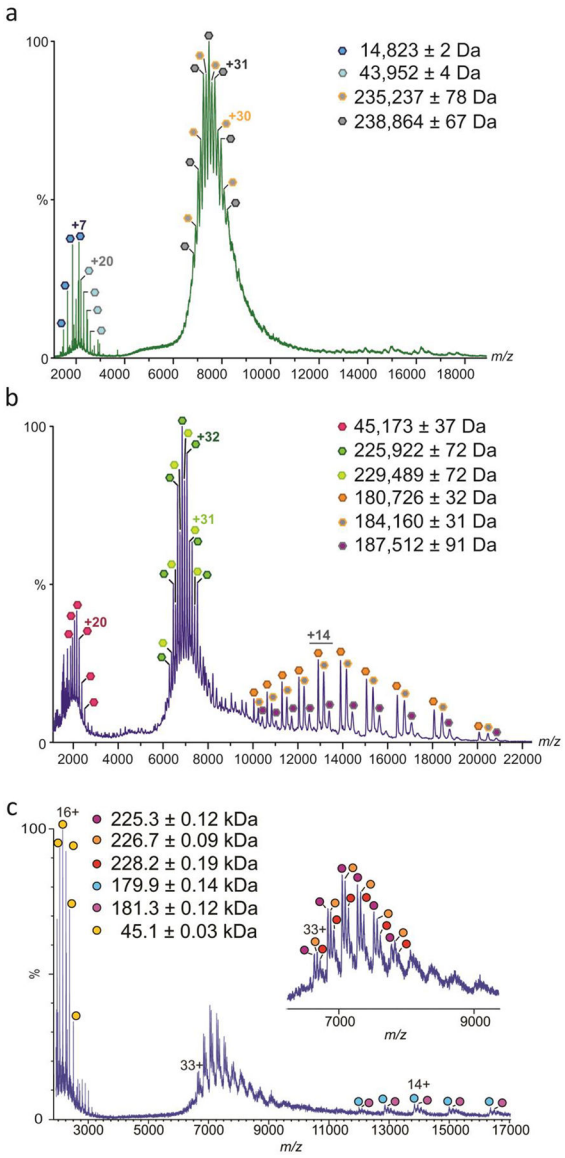

Figure 2.

Non-denaturing mass spectrometry of EcMscL C-GFP and MtMscL C-GFP extracted and purified in the detergent DDM. **a**, Mass spectrum of EcMscL C-GFP collisionally activated with argon gas measures pentameric complexes bound to several adducts. Two different monomeric masses are observed in the low *m/z* region (1,500–3,000 *m/z*) as a result of collisional activation; one corresponding to the expected MtMscL C-GFP fusion protein and the second corresponding to endogenous EcMscL with the initiating methionine removed. Reported in the inset of each mass spectrum is the measured mass and standard deviation. Use of a mscL knock-out strain (Laganowsky et al., 2014) eradicated endogenous MscL contamination. **b**, Mass spectrum of MtMscL C-GFP collisionally activated with sulphur hexafluoride gas reveals up to three bound adducts, with an average mass of ~3.6 kDa, bound to the pentamer and the collisionally dissociated tetramer. Removal of the C-GFP fusion with the TEV protease did not result in reduction of bound LPS. **c**, MtMscL C-GFP

was overexpressed in ClearColi® *E. coli* strain (Lucigen) and analyzed by non-denaturing mass spectrometry.

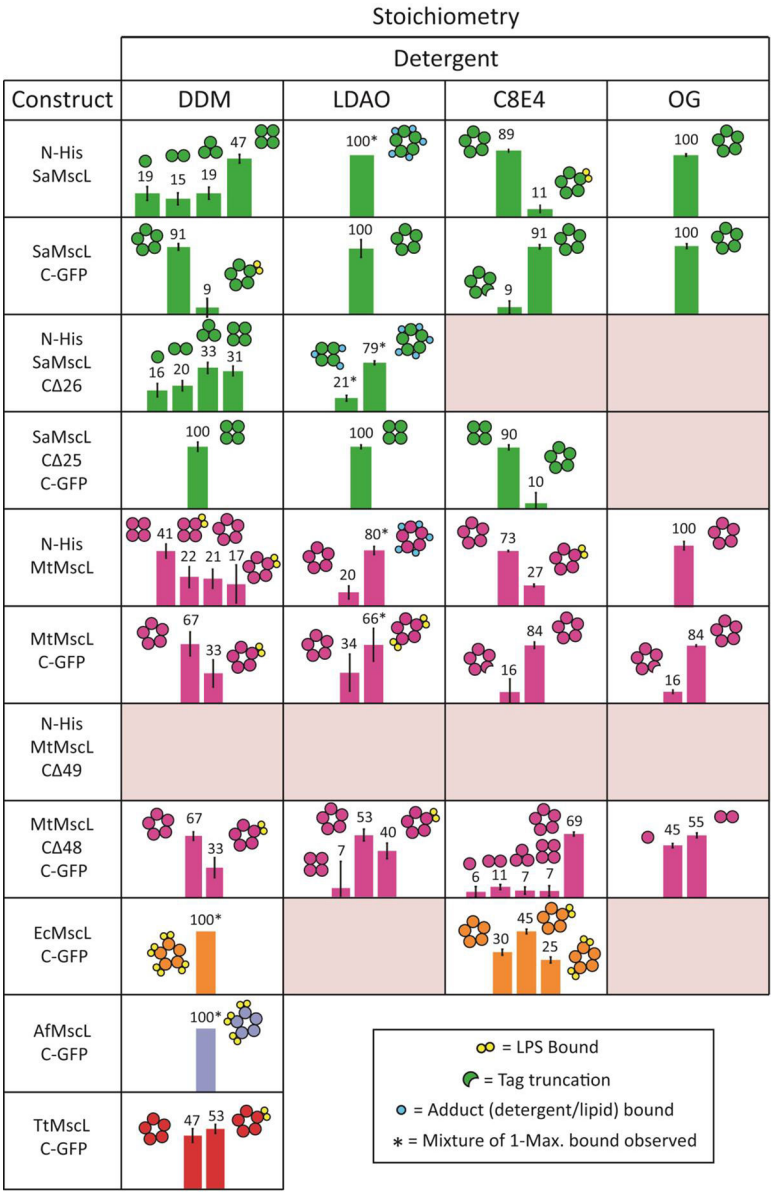

Figure 3.

Stoichiometry and relative abundance of MscL constructs purified in different detergents. All constructs were kept at 4 °C before analysis. All MscL constructs were solubilized, purified and analyzed by non-denaturing mass spectrometry in the same detergent; where fractions from a single peak from size exclusion chromatography was used for non-denaturing mass spectrometry analysis (see Experimental procedures). Cases where the mass spectrum was unresolved or could not be acquired are denoted with a pink box. The relative abundances and fitting errors for the oligomers were calculated using an in-house deconvolution software package using an algorithm described in (Marty et al., 2015). Relative abundances of the different oligomers were calculated by adjusting the mass spectra intensity for detector efficiency (Ebong et al., 2011; Fraser, 2002; Stengel et al., 2012) and assuming that the ionization efficiencies of the various oligomers are similar. All mass

spectra and spectral deconvolution fits are shown in the Table S1 and Supplemental Figures S4–6.

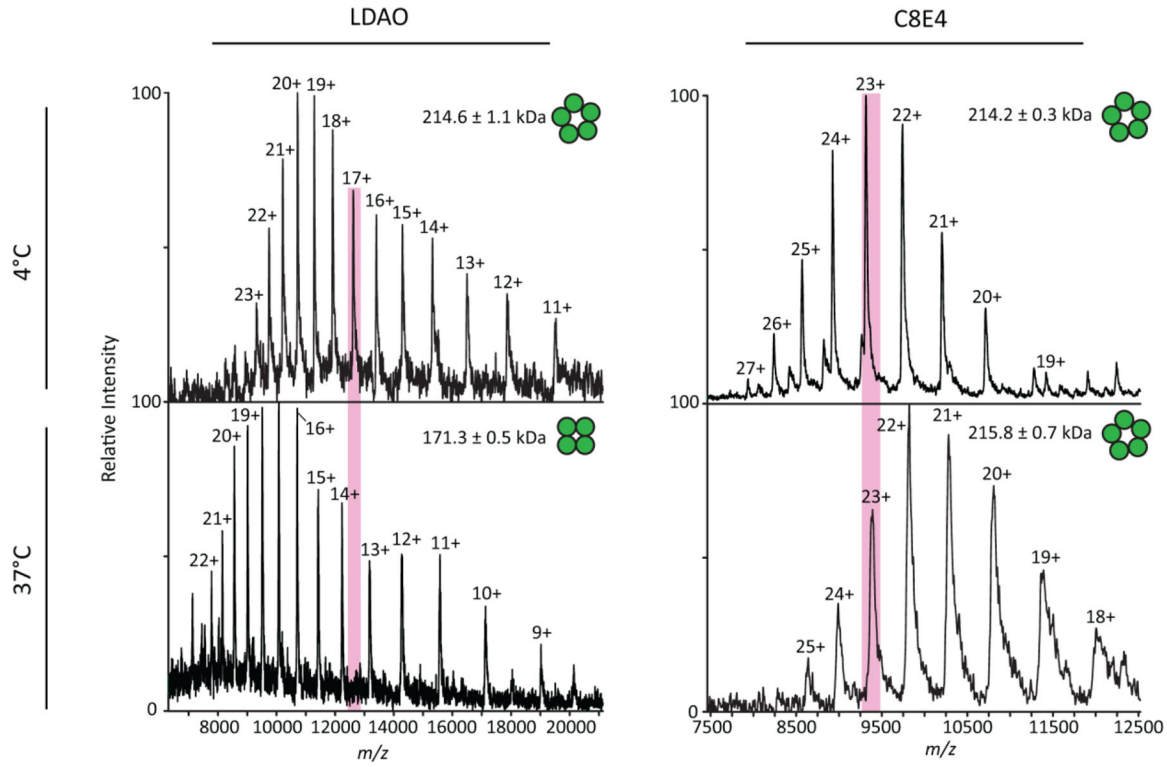

Figure 4.

Oligomeric state of SaMscL C-GFP is dependent on both temperature and solubilizing detergent. Mass spectra of SaMscL C-GFP purified at 4 °C in either LDAO or C8E4 (top panel) prior to incubation at 37 °C for one hour (bottom panel).

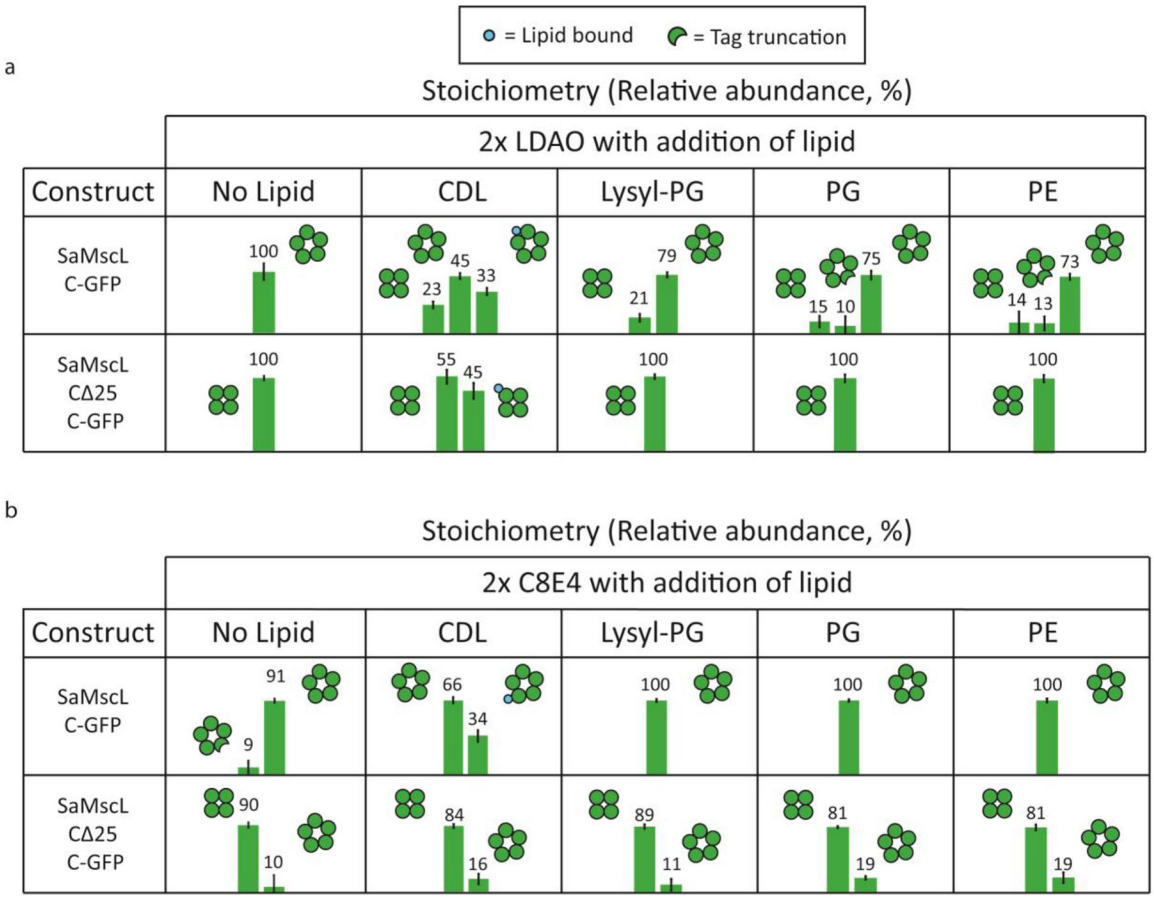

Figure 5.

Stoichiometry of SaMscL constructs in different detergent-lipid environments. After addition of lipid to purified SaMscL constructs, the solution was left at 4 °C for 6 hours before analysis by non-denaturing mass spectrometry (equipped with altered accelerating voltages for increased collisional activation that enabled detergent and lipid removal, whilst keeping oligomeric interaction intact (Hopper et al., 2013)). Protein degradation (loss of C-GFP tagged unit) varied for different mixtures. The relative abundances and fitting errors for the oligomers were calculated using an in-house deconvolution software package using an algorithm described in (Marty et al., 2015). Relative abundances of the different oligomers were calculated by adjusting the mass spectra intensity for detector efficiency (Ebong et al., 2011; Fraser, 2002; Stengel et al., 2012) and assuming that the ionization efficiencies of the various oligomers are similar. All mass spectra and spectral deconvolution fits are shown in the Tables S2 and Supplemental Figures S7–8.

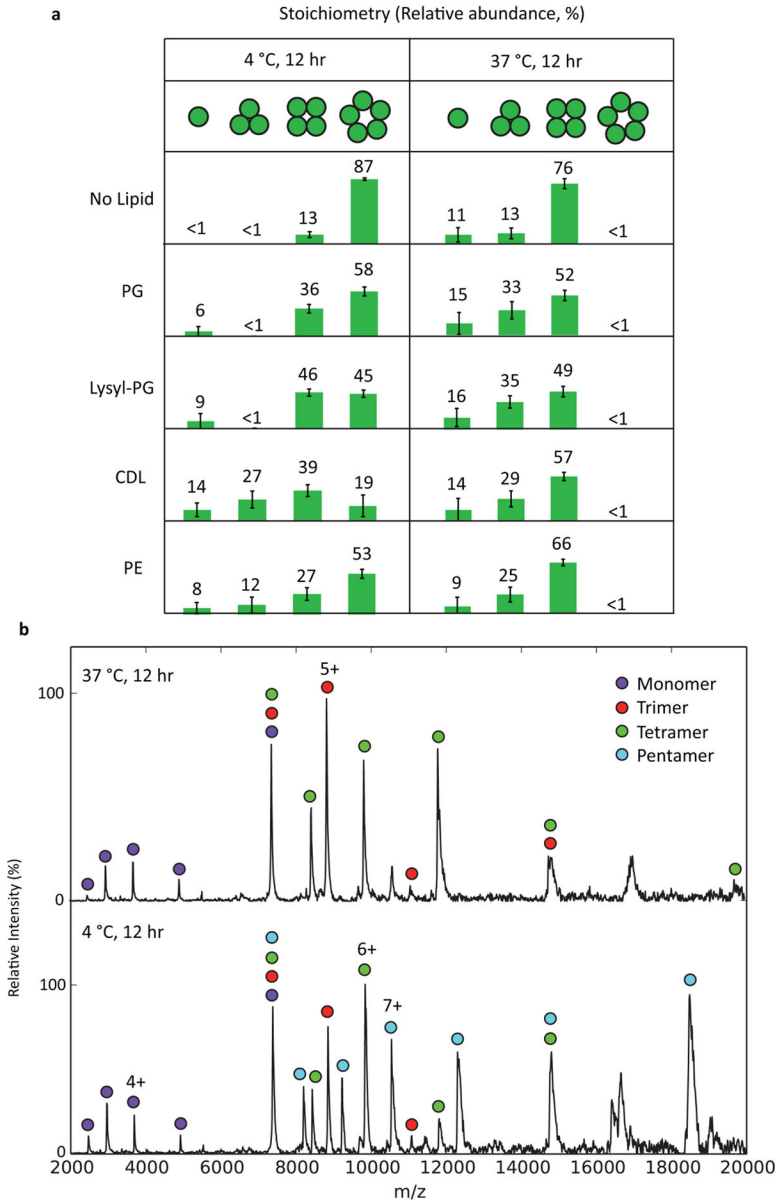

Figure 6.

Detergent-lipid environments influence the temperature induced inter-conversion of SaMscL. **a**, Summary of the effect of lipid addition on temperature-induced oligomer dissociation within LDAO detergent. SaMscL was expressed and purified in LDAO as SaMscL C-GFP and the tag removed by TEV protease cleavage. The protein was analyzed after 12 hours at 4 °C or 37 °C in the presence of 2x the critical micelle concentration of LDAO detergent under equivalent non-denaturing mass spectrometry conditions (equipped with altered accelerating voltages for increased collisional activation that enabled detergent and lipid removal, whilst keeping oligomeric interaction intact (Hopper et al., 2013)). <1 = Negligible amount observed in spectrum. The relative abundances and fitting errors for the oligomers were calculated using an in-house deconvolution software package using an algorithm described in (Marty et al., 2015). Relative abundances of the different oligomers

were calculated by adjusting the mass spectra intensity for detector efficiency (Ebong et al., 2011; Fraser, 2002; Stengel et al., 2012) and assuming that the ionization efficiencies of the various oligomers are similar. All mass spectra and spectral deconvolution fits are shown in the Tables S3 and Supplemental Figure S9. **b**, Representative mass spectrum for PE addition to SaMscL in LDAO for two different temperatures regimes. Monomer (purple), trimer (red), tetramer (green) and pentamer (blue) charge series are represented by filled circles.

Table 1.

Summary and abbreviations for MscL constructs: *Staphylococcus aureus* (Sa), *Mycobacterium tuberculosis* (Mt), *Escherichia coli* (Ec), *Acidithiobacillus ferrooxidans* (Af) and *Thermus thermophilus* (Tt).

Vector Construct	Abbreviation	Theoretical molecular weight (Da)
pet15b-SaMscL-S-TEV-GFP-6xHis	SaMscL C-GFP	42751.9
pet15b-SaMscL CΔ(96–120)-S-TEV-GFP-6xHis	SaMscL CΔ25 C-GFP	39844.5
pet15b-10xHis-Thrombin-SaMscL	N-His SaMscL	15779.6
pet15b-10xHis-Thrombin-SaMscL CΔ(95–120)	N-His SaMscL CΔ26	12743.2
pet15b-MtMscL-S-TEV-GFP-6xHis	MtMscL C-GFP	45296.3
pet15b-MtMscL CΔ(103–151)-S-TEV-GFP-6xHis	MtMscL CΔ48 C-GFP	40077.6
pet15b-10xHis-Thrombin-MtMscL-PG	N-His MtMscL	18440.1
pet15b-10xHis-Thrombin-MtMscL CΔ(102–151)	N-His MtMscL CΔ49	13075.4
pet15b-EcMscL-TEV-GFP-6xHis	EcMscL C-GFP	44076.4
pet15b-AfMscL-TEV-GFP-6xHis	AfMscL C-GFP	45354.0
pet15b-TtMscL-TEV-GFP-6xHis	TtMscL C-GFP	42778.8